

Selective detection of glutathione based on the recovered fluorescence of BSA-AuNCs/Cu²⁺ system

Yining Zhu², Wang Li¹, Cheng Ju¹, Xiang Gong¹, Wenhao Song¹, Yu Zhao¹, Ruijun Li¹ ✉

¹Department of Analytical Chemistry, China Pharmaceutical University, Nanjing 210009, People's Republic of China

²Nanjing No. 13 High School, Nanjing 210000, People's Republic of China

✉ E-mail: ccjlrj@cpu.edu.cn

Published in *Micro & Nano Letters*; Received on 10th December 2018; Revised on 7th March 2019; Accepted on 3rd April 2019

A bovine serum albumin-stabilised gold nanoclusters/Cu²⁺ (BSA-Au NCs/Cu²⁺) system was constructed as a fluorescent sensor for the 'off-on' detection of glutathione (GSH). The fluorescence of BSA-Au NCs could be effectively quenched by Cu²⁺ due to the strong affinity between BSA-Au NCs and Cu²⁺. Then, coordination of Cu²⁺ to GSH enabled the recovery of the fluorescence of BSA-Au NCs. To assess the selectivity of the BSA-Au NCs/Cu²⁺ for GSH, K⁺, Mg²⁺, Ca²⁺, glucose, cysteine, tryptophan, and phenylalanine were examined under identical conditions, and all of them did not induce noticeable responses to BSA-Au NCs/Cu²⁺ except for Cys. There was a good linear dependence of fluorescence intensity on the concentration of GSH in the range of 0.4–20.0 μM with the detection limit of 0.36 μM. The proposed sensor showed excellent performance in the selective detection of GSH.

1. Introduction: Glutathione (GSH), a paramount thiol in mammalian and eukaryotic cells, plays a critical role in combating oxidative stress and maintaining redox homeostasis that is pivotal for cell growth and function, such as intracellular signal transduction, protein and DNA synthesis, cytokine production and immune response [1, 2]. Generally, an abnormal level of GSH is associated with many diseases including Alzheimer's, Parkinson's and coronary heart disease and lung damage [3, 4]. Owing to the biological and clinical importance of GSH, it is meaningful to develop an effective analytical method for the detection of GSH with rapid response time, good selectivity and sensitivity.

Hitherto, various methods have been established for the detection of GSH, such as high performance liquid chromatography (HPLC) [5], surface-enhanced Raman scattering (SERS) [6], electrochemistry [7], capillary electrophoresis [8], mass spectrometry [9] and fluorescence spectroscopy [10–12]. Among them, fluorescence spectroscopy is rather promising due to its high sensitivity and real-time monitoring.

Up to now, many fluorescent probes and sensors have been reported for the detection of GSH, including organic fluorophores [13], nanocomposite [14, 15] and quantum dots (QDs) [16, 17], but many of them need complex synthetic strategies and operation, expensive reagents consumption and time-consuming. Therefore, the choice of fluorescent sensors with favourable fluorescence properties in a high selective, simple preparation, low cost, and easy operations, is the key issue. Gold nanoclusters (Au NCs) have drawn increasing attention due to its unique optical properties and excellent chemical or biomedical application [18, 19]. Au NCs prepared by the microwave-assisted protocol exhibit many advantages, such as simple synthesis, low cost, and strong red fluorescence emission [20]. Additionally, bovine serum albumin (BSA), as both the stabilising and reducing agent, has been widely applied in Au NC-based fluorescent systems [21, 22].

The detection mechanism mainly relied on the fluorescence resonance energy transfer between the fluorescent probe and other nanomaterials, such as MnO₂ nanosheet [14, 23]. However, the preparation process of nanomaterials was complicated. In addition, Han [16] demonstrated that the fluorescence of CdTe QDs was quenched greatly by Hg²⁺, and the fluorescence was recovered in the presence of biothiols. Tian [24] demonstrated that Hg²⁺ could quench the excellent fluorescence of Au NCs, which was used as a fluorescent sensor for the detection of GSH. However,

the strong toxicity especially Hg²⁺ restricted their extensive application. Fortunately, Cu²⁺ ion, which shows lower toxicity than Hg²⁺, could be served as an ideal alternative quencher for GSH detection [2].

Herein, a BSA-Au NCs/Cu²⁺ system has been constructed for the selective detection of GSH. The strong fluorescence of BSA-Au NCs can be effectively quenched by Cu²⁺ to form an 'on-off' BSA-Au NCs/Cu²⁺ system. Also, the quenched fluorescence of BSA-Au NCs/Cu²⁺ could be restored subsequently by addition of GSH, achieving the 'off-on' process. The as-prepared fluorescent sensor with the advantages in high selective, simple preparation, low cost, and easy operations, showed great superiority in the detection of GSH.

2. Experimental

2.1. Chemicals and reagents: Chloroauric acid (HAuCl₄·4H₂O, 47.8%) was obtained from Shanghai Chemical Reagent Company (China). BSA was obtained from Beijing Solarbio Science & Technology Co., Ltd (China). CuSO₄ was purchased from Shanghai Xinbao Fine Chemical Factory (Shanghai). Cysteine (Cys), tryptophan (Trp) and phenylalanine (Phe) were provided by Aladdin Chemistry Co. Ltd (Shanghai). KCl, MgCl₂, CaCl₂, GSH, and glucose were obtained from Aladdin Industrial Corporation (China).

2.2. Instruments and apparatus: Microwave heating was achieved in a P70D20P (WO) microwave oven (China). All of the fluorescence emission spectra were recorded with a Horiba Jobin Yvon Fluoromax-4 spectrofluorometer (France). Fluorescence microscopy images were obtained on an IX53 Olympus (Japan).

2.3. Preparation of the BSA-Au NCs: The BSA-Au NCs were synthesised by a microwave-assisted method according to the reported references with some modification [25, 26]. Au(III) ions were added to the aqueous BSA solution, the reduction ability of BSA molecules was then activated and entrapped Au(III) ions. The BSA coating layer on Au NCs also facilitated post synthesis surface modifications with functional ligands. 1.00 ml of 5 mM HAuCl₄ solution was added dropwise to 1.00 ml of 25 mg/ml BSA solution and stirred 3 min. Subsequently, the obtained solution was adjusted to pH 12 with 1.0 M NaOH solution. Then, the solution mixture was heated with a microwave oven at 180 W

for 4 min, followed by a 4 min pause and another 4 min heating (180 W). Finally, the resultant BSA-Au NCs was added up to 2 ml and stored at 4°C prior to use.

2.4. Procedures for GSH determination: To achieve the ‘off-on’ fluorescent detection, 30 µl of 0.5 mg/ml Cu²⁺ was firstly added into the BSA-Au NCs (20 µl) solution, and the mixed solution was incubated for 5 min. Afterwards, various amounts of GSH reacted with the mixture in 100 µl of 10 mM phosphate buffer saline (PBS; pH 7.1) for 10 min. The corresponding fluorescence spectra were determined at room temperature with an excitation wavelength at 470 nm. Under optimised conditions, K⁺, Mg²⁺, Ca²⁺, glucose, Cys, Trp, and Phe were chosen to evaluate the selectivity of the sensor.

3. Results and discussion

3.1. Characterisation of BSA-Au NCs: The optical properties of the BSA-Au NCs were investigated by several characterisation methods. Upon excitation at 470 nm, the BSA-Au NCs indicated an intensive fluorescence emission with a sharp peak centred at ~644 nm (Fig. 1). The suspension was emitted a red fluorescence under an ultraviolet (UV) lamp at 365 nm. Moreover, the red clusters could be observed apparently under a fluorescence microscope (Fig. 1, inset picture).

3.2. Fluorescence quenching of the BSA-Au NCs by Cu²⁺: It is well known that Cu²⁺, which is a paramagnetic ion with an unfilled d shell, could quench the fluorescence through electron or energy transfer [27]. Therefore, we chose Cu²⁺ as a quencher for the quenching of the excellent fluorescence of BSA-Au NCs, and then fabricated the BSA-Au NCs/Cu²⁺ system. The different concentration of Cu²⁺ and the influence of incubation time were taken into consideration. The quenching effect of Cu²⁺ on the BSA-Au NCs fluorescence was investigated by adding increasing amounts of Cu²⁺ into BSA-Au NCs solution. Finally, 20 µl BSA-Au NCs and 30 µl of Cu²⁺ stock solution (0.5 mg/ml) were added to the colorimetric tube and adjusted to 250 µl with PBS solution. The results showed that the intensity of BSA-Au NCs/Cu²⁺ (Fig. 2b) was much less than that of BSA-Au NCs (Fig. 2a), and the quenching efficiency was up to 48.8%. The quenching efficiency was calculated using (1)

$$\text{Eff}_q(\%) = (F_0 - F)/F_0 \quad (1)$$

where F_0 and F were the fluorescence intensity of BSA-Au NCs in the absence and presence of Cu²⁺, respectively; Eff_q was the fluorescence quenching efficiency of Cu²⁺.

To enhance the performance of the BSA-Au NCs/Cu²⁺ system for the detection of GSH, PBS was optimised in the range

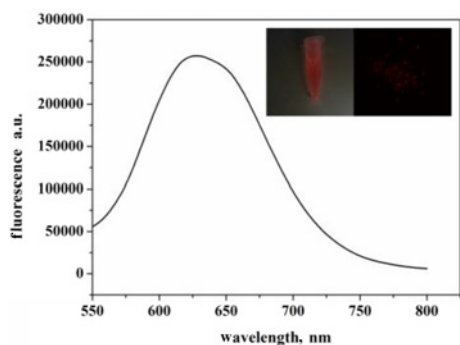


Fig. 1 Fluorescence emission spectrum of BSA-Au NCs; Inset pictures: photographs of BSA-Au NCs under UV lamp at 365 nm (left) and fluorescent microscopy image (right)

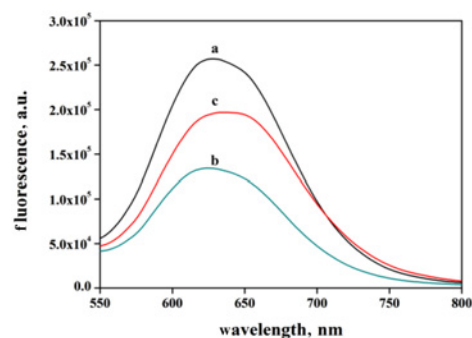


Fig. 2 Fluorescence spectra of
a BSA-Au NCs
b BSA-Au NCs/Cu²⁺, and
c BSA-Au NCs/Cu²⁺/GSH ($\lambda_{\text{ex}}=470$ nm; Cu²⁺: 0.06 mg/ml; GSH: 20 µM)

of pH 6.7–7.4. The results (Fig. 3a) showed that the quenching effect reinforced firstly and then decreased with the increasing of pH. The sensor exhibited a high quenching effect at pH 7.1.

The influence of incubation time on the quenching efficiency of Cu²⁺ was considered. 20 µl BSA-Au NCs and 30 µl of Cu²⁺ stock solution (0.5 mg/ml) were added to the colorimetric tube and adjusted to 250 µl with PBS solution (pH 7.1). A series of incubation times (1–20 min) were studied in this work. The results (Fig. 3b) showed that the quench reaction between BSA-Au NCs and Cu²⁺ reached equilibrium during 1–10 min, revealing a relative rapid reaction between BSA-Au NCs and Cu²⁺ at room temperature.

Therefore, to construct the BSA-Au NCs/Cu²⁺ system, 20 µl BSA-Au NCs and 30 µl of 0.5 mg/ml Cu²⁺ were chosen for the quench reaction with an incubation time of 5 min at pH 7.1

3.3. Fluorescence restoration for GSH detection: The interaction between BSA-Au NCs and Cu²⁺ was disturbed by the addition of GSH subsequently, resulting in restored fluorescence of BSA-Au NCs. The influence of incubation time on the fluorescence recovery efficiency was also considered. A series of incubation times (2, 5, 10, 15, 20, 25, 30 min) were studied in this work. The results (Fig. 4) suggested the fluorescence restored remarkably at the incubation time of 10 min in the presence of GSH.

Under identical conditions, the results (Fig. 2c) showed that the fluorescence intensity recovered to the intensity of 79.0% of the BSA-Au NCs when the concentration of GSH was 20 µM. Also, the fluorescence intensity increased 1.5-fold relative to the BSA-Au NCs/Cu²⁺ system. The as-prepared BSA-Au NCs/Cu²⁺ system was used for quantitative detection of GSH. GSH with various concentrations was added to the BSA-Au NCs/Cu²⁺

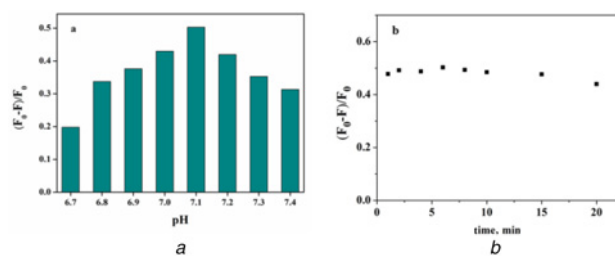


Fig. 3 The performance of fluorescence quenching of BSA-Au NCs/Cu²⁺ system with
a different pH solutions (10 mM PBS buffer)
b different incubation time in the presence of Cu²⁺ ($\lambda_{\text{ex}}=470$ nm; Cu²⁺: 0.06 mg/ml)

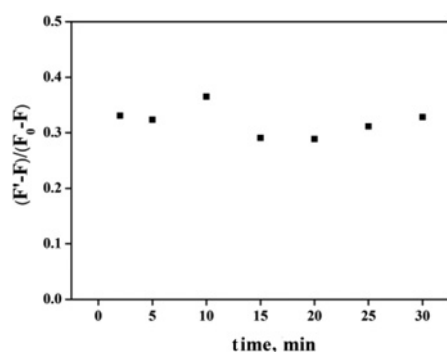


Fig. 4 Relationship between the fluorescent intensity of the quenched BSA-Au NCs/Cu²⁺ system and incubation time of restoration in the presence of GSH ($\lambda_{ex} = 470$ nm; Cu²⁺: 0.06 mg/ml; GSH: 20 μ M)

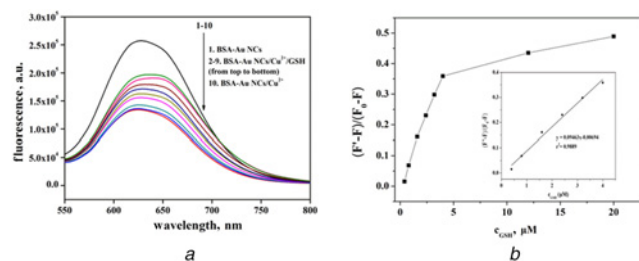


Fig. 5 The relationship of the quenched BSA-Au NCs/Cu²⁺ system with the different concentrations of GSH
a fluorescence responses of different concentrations of GSH (2-9 from top to bottom: 20.0, 12.0, 4.0, 3.2, 2.4, 1.6, 0.8 and 0.4 μ M)
b the linear relationship of different concentrations of GSH and $(F' - F)/(F_0 - F)$

solutions to assess the sensitivity. The fluorescence intensity increased successively in the GSH concentration range from 0.4 to 20.0 μ M, whereas the maximum emission wavelengths and spectral widths did not show an obvious change. The fluorescence response curves were shown in Fig. 5*a*. The fluorescence recovery efficiency could be described by (2)

$$\text{Eff}_r(\%) = (F' - F)/(F_0 - F) \quad (2)$$

where F' was the recovered fluorescence intensity of the BSA-Au NCs in the presence of GSH. Eff_r was the fluorescence recovery efficiency of GSH.

As shown in Fig. 5*b*, there was a well plotted linear relationship between $((F' - F)/(F_0 - F))$ and the concentration of GSH (c_{GSH}) ranging from 0.4 to 20.0 μ M. The curve followed the standard regression equation $(F' - F)/(F_0 - F) = -0.00694 + 0.09463 c_{\text{GSH}}$ ($r = 0.9944$). The limit of detection (LOD) was ~ 0.36 μ M, calculated by the generalised 3σ method. The results suggested a superior performance of this sensor for GSH detection.

3.4. Selectivity and application evaluation of the 'off-on' sensor: 20 μ M K⁺, Mg²⁺, Ca²⁺, Hg²⁺, glucose, Cys, Trp, and Phe were examined under optimised conditions to assess the selectivity of the BSA-Au NCs/Cu²⁺ system for the detection of GSH. As it clearly could be found in Fig. 6, all of them did not exhibit significant interference on the detection performance of GSH except for Cys. These phenomena indicated that the BSA-Au NCs/Cu²⁺ system responded to GSH with high selectivity. To inspect the accuracy of the system, different concentrations of GSH (1.00, 3.00, 5.00 μ M) were spiked into the water samples without any treatment. Other procedures were the same as described above.

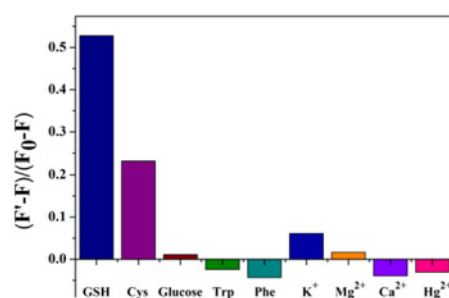


Fig. 6 Selectivity of the BSA-Au NCs/Cu²⁺ system for GSH and other analytes ($\lambda_{ex} = 470$ nm; Cu²⁺: 0.06 mg/ml; GSH: 20 μ M)

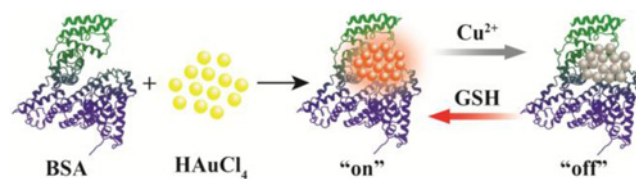


Fig. 7 Schematic representation of fabrication of BSA-Au NCs/Cu²⁺ system and its application for detection of GSH

The recoveries were in the range of 97.4–103% and the relative standard deviations were all <4.5%. We also determined the GSH in tomato samples. Tomato was homogenised, and then 45.0 g homogenate was weighed. After centrifuging at 4500 rpm for 2 min, the supernatant of 6.5 ml was filtered through 0.45 μ m pore size cellulose acetate membrane and diluted ten times with water [28]. The average concentration of GSH in tomato detected by the sensor was 1.45×10^2 μ g/l. In addition, we carried on the recovery measurement by spiking 1.62×10^2 μ g/l GSH to guarantee the sample test's accuracy. The recoveries of GSH in tomato were 90.0–108.7%. The results supported the proposed method in the application of practical samples.

3.5. Mechanism of proposed fluorescent sensor: The process for the synthesis and the application of the BSA-Au NCs/Cu²⁺ system in GSH detection was illustrated in Fig. 7. When the paramagnetic Cu²⁺ chelated with glycine in the BSA chain (BSA-Au NCs/Cu²⁺ complex), the excited electron of the BSA-Au NCs lost its energy due to the intersystem crossing. Consequently, the fluorescence of BSA-Au NCs was quenched after combining with Cu²⁺, giving rise to the 'on-off' process [29]. However, Cu²⁺, as a thiophilic metal ion has a particular binding preference to GSH because of the several potential coordinating sites of GSH, such as sulphhydryl, carboxyls, and amino group [30]. Therefore, Cu²⁺ formed a more stable complex with GSH than BSA-Au NCs. Cu²⁺ was released from the surface of BSA-Au NCs, which led to the restoration of fluorescence of BSA-Au NCs, 'off-on' process achieved.

3.6. Comparison with other methods: In comparison with other fluorescent probes, the BSA-Au NCs/Cu²⁺ system has some advantages. As can be seen in Table 1, most heavy metals were toxic and their long-term body accumulation may cause serious illnesses. Also, the BSA-Au NCs/Cu²⁺ system was much safer. Some reported methods [5, 11] presented low selectivity for the determination of GSH because they detected other analyses simultaneously. We also obtained a lower detection limit compared with previously reported methods [14, 31, 32]. Previous studies usually used materials with heavy metal ions (such as mercury ion) or MnO₂ nanoparticles to detect GSH [14, 24, 33].

Table 1 Comparison with previously reported methods for determination of GSH

Material used	Methods	Analyte	Time, min	LOD, μM	Ref.
—	HPLC	GSH	5.1	0.0005	[5]
—	SERS	glutathione disulfide (GSSG)	—	—	—
—	electrochemistry	GSH	20	1	[31]
—	fluorescent probes	GSH	—	3	[32]
MCQ-O-NBD	fluorescent probes	Cys	15	0.006	[11]
GO-MnO ₂ -FL		GSH	—	—	—
N-acetyl-L-cysteine (NAC)-capped CdTe QD-Hg(II)		GSH	360	1.53	[14]
Au NC-Hg(II)		GSH	—	0.24	[33]
BSA-AuNCs/Cu ²⁺		GSH	20	0.007	[24]
		homocysteine (Hcy)	15	0.36	the work

4. Conclusions: In summary, we designed and constructed an 'off-on' fluorescent sensor for the determination of GSH based on the BSA-Au NCs/Cu²⁺ system. The results demonstrated that the sensor could serve as an efficient method for the detection of GSH. The proposed method exhibited high selectivity and sensitivity with a linear range of 0.4–20.0 μM ($(F' - F)/(F_0 - F) = 0.00469 - 0.09463 c_{\text{GSH}}$ ($r = 0.9944$)). Therefore, the novel sensor would show great potential to act as a useful tool in real sample analysis and biological investigation.

5. Acknowledgment: This work was financially supported by the National Natural Science Foundation of China (grant no. 21804141).

6 References

- Lu S.C.: 'Regulation of glutathione synthesis', *Mol. Aspects Med.*, 2009, **30**, pp. 42–59
- Yang C.L., Wang X., Liu H.Y., *ET AL.*: 'On-off-on fluorescence sensing of glutathione in food samples based on a graphitic carbon nitride (g-C₃N₄)-Cu²⁺ strategy', *New. J. Chem.*, 2017, **41**, pp. 3374–3379
- Pocernich C.B., Butterfield D.A.: 'Elevation of glutathione as a therapeutic strategy in Alzheimer disease', *Biophys. Acta*, 2012, **1822**, pp. 625–630
- Wu G., Fang Y.Z., Yang S., *ET AL.*: 'Glutathione metabolism and its implications for health', *J. Nutr.*, 2004, **134**, (3), pp. 489–492
- McDermott G.P., Francis P.S., Holt K.J., *ET AL.*: 'Determination of intracellular glutathione and glutathione disulfide using high performance liquid chromatography with acidic potassium permanganate chemiluminescence detection', *Analyst*, 2011, **136**, pp. 2578–2585
- Saha A., Jana N.R.: 'Detection of cellular glutathione and oxidized glutathione using magnetic-plasmonic nanocomposite-based 'turn-off' surface enhanced Raman scattering', *Anal. Chem.*, 2013, **85**, pp. 9221–9228
- Gao W.Y., Liu Z.Y., Qi L.M., *ET AL.*: 'Ultrasensitive glutathione detection based on lucigenin cathodic electrochemiluminescence in the presence of MnO₂ nanosheets', *Anal. Chem.*, 2016, **88**, pp. 7654–7659
- Hodáková J., Preisler J., Foret F., *ET AL.*: 'Sensitive determination of glutathione in biological samples by capillary electrophoresis with green (515 nm) laser-induced fluorescence detection', *J. Chromatogr. A*, 2015, **1391**, pp. 102–108
- Burford N., Eelman M.D., Mahony D.E., *ET AL.*: 'Definitive identification of cysteine and glutathione complexes of bismuth by mass spectrometry: assessing the biochemical fate of bismuth pharmaceutical agents', *Chem. Commun.*, 2002, **9**, pp. 146–147
- Tang B., Xing Y.L., Li P., *ET AL.*: 'A rhodamine-based fluorescent probe containing a Se–N bond for detecting thiols and its application in living cells', *J. Am. Chem. Soc.*, 2007, **129**, p. 11666
- Ren X.J., Tian H.H., Yang L., *ET AL.*: 'Fluorescent probe for simultaneous discrimination of Cys/Hcy and GSH in pure aqueous media with a fast response under a single-wavelength excitation', *Sens. Actuators B, Chem.*, 2018, **273**, pp. 1170–1178
- Yin J., Kwon Y., Kim D., *ET AL.*: 'Cyanine-based fluorescent probe for highly selective detection of glutathione in cell cultures and live mouse tissues', *J. Am. Chem. Soc.*, 2014, **136**, pp. 5351–5358
- Ji X., Lv M.H., Pan F.C., *ET AL.*: 'A dual-response fluorescent probe for the discrimination of cysteine from glutathione and homocysteine', *Spectrochim. Acta A*, 2019, **206**, pp. 1–7
- Guo Y.X., Zhang X.D., Wu F.G.: 'A graphene oxide-based switch-on fluorescent probe for glutathione detection and cancer diagnosis', *J. Colloid Interface Sci.*, 2018, **530**, pp. 511–520
- Zhai Q.F., Xing H.H., Fan D.Q., *ET AL.*: 'Gold-silver bimetallic nanoclusters with enhanced fluorescence for highly selective and sensitive detection of glutathione', *Sens. Actuators B, Chem.*, 2018, **273**, pp. 1827–1832
- Han B.Y., Yuan J.P., Wang E.K.: 'Sensitive and selective sensor for biothiols in the cell based on the recovered fluorescence of the CdTe quantum dots–Hg(II) system', *Anal. Chem.*, 2009, **81**, pp. 5569–5573
- Gupta A., Verma N.C., Khan S., *ET AL.*: 'Carbon dots for naked eye colorimetric ultrasensitive arsenic and glutathione detection', *Biosens. Bioelectron.*, 2016, **81**, pp. 465–472
- Chen L.Y., Wang C.W., Yuan Z., *ET AL.*: 'Fluorescent gold nanoclusters: recent advances in sensing and imaging', *Anal. Chem.*, 2015, **87**, pp. 216–229
- Nie L., Xiao X., Yang H.: 'Preparation and biomedical applications of gold nanocluster', *Chemistry*, 2015, **16**, pp. 8164–8175
- Yan L., Cai Y.Q., Zheng B.Z., *ET AL.*: 'Microwave-assisted synthesis of BSA-stabilized and HSA-protected gold nanoclusters with red emission', *J. Mater. Chem.*, 2012, **22**, pp. 1000–1006
- Li H.W., Yue Y., Liu T.Y., *ET AL.*: 'Fluorescence-enhanced sensing mechanism of BSA-protected small gold-nanoclusters to silver(I) ions in aqueous solutions', *J. Phys. Chem. C*, 2013, **117**, pp. 16159–16165
- Cui M.L., Liu J.M., Wang X.X., *ET AL.*: 'A promising gold nanocluster fluorescent sensor for the highly sensitive and selective detection of S²⁻', *Sens. Actuators B, Chem.*, 2013, **188**, pp. 53–58
- Wang Y., Jiang K., Zhu J., *ET AL.*: 'A FRET-based carbon dot–MnO₂ nanosheet architecture for glutathione sensing in human whole blood samples', *Chem. Commun.*, 2015, **51**, pp. 12748–12751
- Tian D., Qian Z., Xia Y., *ET AL.*: 'Gold nanocluster-based fluorescent probes for nearinfrared and turn-on sensing of glutathione in living cells', *Langmuir*, 2012, **28**, pp. 3945–3951
- Hsu N.Y., Lin Y.W.: 'Microwave-assisted synthesis of bovine serum albumin–gold nanoclusters and their fluorescence-quenched sensing of Hg²⁺ ions', *New. J. Chem.*, 2015, **40**, pp. 1155–1161
- Xie J.P., Zheng Y.G., Ying J.Y.: 'Protein-directed synthesis of highly fluorescent gold nanoclusters', *J. Am. Chem. Soc.*, 2009, **131**, pp. 888–889
- Krämer R.: 'Fluorescent chemosensors for Cu²⁺ ions: fast, selective, and highly sensitive', *Angew. Chem. Int. Ed.*, 1998, **37**, pp. 772–773
- Yan N., Zhu Z.F., Ding N., *ET AL.*: 'In-line preconcentration of oxidized and reduced glutathione in capillary zone electrophoresis using transient isotachopheresis under strong counter-electroosmotic flow', *J. Chromatogr. A*, 2009, **1216**, pp. 8665–8670
- Durgadas C.V., Sharma C.P., Sreenivasan K.: 'Fluorescent gold clusters as nanosensors for copper ions in live cells', *Analyst*, 2011, **136**, pp. 933–940

- [30] Shi Y.P., Pan Y., Zhang H., *ET AL.*: 'A dual-mode nanosensor based on carbon quantum dots and gold nanoparticles for discriminative detection of glutathione in human plasma', *Biosens. Bioelectron.*, 2014, **56**, pp. 39–45
- [31] Huang G.G., Hossain M.K., Han X., *ET AL.*: 'A novel reversed reporting agent method for surface-enhanced Raman scattering; highly sensitive detection of glutathione in aqueous solutions', *Analyst*, 2009, **134**, pp. 2468–2474
- [32] Karuwan C., Wisitsoraat A., Chaisuwan P, *ET AL.*: 'Screen-printed graphene-based electrochemical sensors for a microfluidic device', *Anal. Methods*, 2017, **9**, pp. 3689–3695
- [33] Wang J., Li D.Q., Liu X.Y., *ET AL.*: 'One-pot synthesis of highly luminescent N-acetyl-L-cysteine-capped CdTe quantum dots and their size effect on the detection of glutathione', *New J. Chem.*, 2018, **42**, pp. 15743–15749